IEEE Access
Multidisciplinary ⋮ Rapid Review ⋮ Open Access Journal

Received 13 September 2023, accepted 8 November 2023, date of publication 16 November 2023,
date of current version 22 November 2023.

Digital Object Identifier 10.1109/ACCESS.2023.3333901

RESEARCH ARTICLE

TLB & WC-TLB-MM: The Improved Min-Max Algorithms for Multi Targets Indoor Localization

FARID YULI MARTIN ADIYATMA[1], DWI JOKO SUROSO[2], AND PANARAT CHERNTANOMWONG[1]

[1]School of Engineering, King Mongkut's Institute of Technology Ladkrabang, Bangkok 10520, Thailand
[2]Department of Nuclear Engineering and Engineering Physics, Universitas Gadjah Mada, Yogyakarta 55281, Indonesia

Corresponding author: Panarat Cherntanomwong (panarat.ch@kmitl.ac.th)

This work was supported by the King Mongkut's Institute of Technology Ladkrabang.

ABSTRACT Internet of Things (IoT)-based Indoor localization is the most commonly used system to determine target locations indoors. It applies to various purposes, e.g., indoor navigation, asset tracking in warehouse management, and tracking people in hospitals. Distance-based techniques using the Received Signal Strength Indicator (RSSI), e.g., Min-Max, are widely applied because they can be directly implemented without prerequisite work such as site surveys. However, a challenging indoor environment with high numbers of interiors and people can obstruct signal propagation. This obstruction can reduce the accuracy of translating RSSI to distance using the path loss model, which will degrade the localization accuracy. In this paper, we introduce two improved Min-Max (MM) algorithms, i.e., Three Layer Bounding Box Min-Max (TLB-MM) and Weighted Centroid TLB-MM (WC-TLB-MM), to alleviate the issue and achieve higher localization accuracy. The novelty of the proposed TLB-MM is incorporating RSSI error functions to generate three-layer bounding boxes: the inner, middle, and outer in the Min-Max algorithm. Meanwhile, WC-TLB-MM enhanced the TLB-MM algorithm by integrating the Weighted Centroid Localization Algorithm (WCLA) in the calculation process. We validate our proposal by conducting various experiments using Wi-Fi at 2.4 GHz deployed in a laboratory room of 10.17 m × 9.12 m. Experimental results demonstrate that TLB-MM improved the accuracy performance to 55.78% and 30.86%, while WC-TLB-MM gave 40.93% and 7.65% compared to Min-Max and WCLA, respectively. From these results, our proposed methods are proven simple yet applicable to RSSI-based indoor localization systems.

INDEX TERMS Indoor localization, distance-based technique, RSSI, min-max (MM), Wi-Fi.

I. INTRODUCTION

The advancement of Internet of Things (IoT) systems in buildings increases a significant opportunity to allow the development of indoor location-based services (ILBS) [1]. These ILBS, relying on target or device location data, enhance the efficiency of daily activities [2]. Thus, accurately determining the target or device's location is imperative. In the outdoor environment, they established a localization system. e.g., the Global Positioning System (GPS) relies on clear signal communication between satellites and devices [3]. However, the utilization of satellite signals encounters difficulty with obstructed propagation caused by walls and interiors, failing to provide high-accuracy localization indoors [4]. Various wireless technologies have been integrated to address the disadvantages of a closed environment into the creation of indoor localization systems designed for purposes such as navigation [5], elder monitoring [6], asset tracking in warehouse management [7], disaster management [8] and tracking people or assets in hospitals [9].

Wireless Fidelity (Wi-Fi) is highlighted as the most promising technology to extend localization systems in indoor environments due to its sensing capabilities, high accuracy, extensive availability of infrastructure, low cost, and less complex setup [10]. For localization purposes, Wi-Fi empowers various parameters, such as Received Signal Strength Indicator (RSSI) [11], Angle of Arrival (AoA) [12], Time of Arrival (ToA) [13], Time Difference of

The associate editor coordinating the review of this manuscript and approving it for publication was Tawfik Al-Hadhrami.

Arrival (TDoA) [14] and Channel State Information (CSI) [15]. Compared to others, RSSI has a valuable advantage due to its ease of extraction, which involves straightforward procedures and does not require additional hardware installation [16].

Generally, the existing RSS-based indoor localization technique can be classified into two types: (1) direct utilization of RSSI (distance-free) or (2) conversion of RSSI to distance information (distance-based) [17]. In the distance-free technique, there is one commonly used technique called fingerprinting. As the name suggests, this technique mimics the human fingerprint identification technique. However, the localization fingerprinting technique relies on a radio map instead of biological fingerprints. This technique is highly favored since it is resistant to multipath fading. The fingerprint technique involves two phases: the offline phase, dedicated to constructing a radio map or fingerprint database, and the online phase, where the localization process occurs, in which target signal parameters are compared to fingerprint databases to infer their location [16]. During the online phase, various pattern matching algorithms are commonly employed, including Euclidean distance [16], nearest neighbor [18], machine and deep learning-based such as K-Nearest Neighbors (KNN) [19], [20], Support Vector Machine (SVM) [21], [22], Convolutional Neural Networks (CNN) [23], [24], [25].

Despite its ease of use and high performance, the fingerprint technique may not be reliably applicable in dynamic environments with frequent changes in layout and high levels of mobility or activities [26]. Moreover, reconstructing or updating the fingerprint database requires significant manual labor, time, and expenses [16]. Contrary to the fingerprint technique, the distance-based approach eliminates the need for constructing a radio map. Instead, it highly depends on RSSI-distance translation between the transmitter or access point (AP) and the receiver or target. The most common method to translate RSSI to distance is utilizing the path loss model, i.e., the log distance model [27].

Several distance-based techniques have been proposed, including trilateration (TRI), Min-Max (MM), and the Weighted Centroid Localization Algorithm (WCLA). The TRI algorithm uses at least three APs as the reference points to create essential mathematical functions with a geometric approach to determine the target location [11], [28], [29], [30]. TRI method employs a geometric approach where three circles are formed with the coordinates of the APs as their anchors, and the distance serves as the radius, calculated from the RSSI-distance translation. This algorithm estimates the target location by identifying the intersection point of these three circles. However, the dynamic nature of the environment poses challenges in using RSSI values to accurately represent the distance between the AP and the target. This challenge may lead to difficulty finding the intersection point, resulting in increased localization errors. The MM algorithm is introduced to fix the intersection-finding problem by approximating the target location using a an interest box instead of an intersection [31], [32]. This interest box is formed by the overlap of at least three bounding boxes generated by adding and subtracting the converted distance from RSSI into the coordinates of APs. Another distance-based algorithm, WCLA, employs the inverse of RSSI-to-distance translation as weights in its computation. By multiplying the coordinates with their respective weights, the algorithm can determine the target's coordinate [33], [34], [35].

Although RSSI offers several advantages, it is also prone to fluctuations due to the multipath signal effect, antenna orientation, and other things with which it interacts, such as interior structures, people, and time [36]. Consequently, RSSI-to-distance translation may not perform consistently because the path loss exponent is not universally applicable in every indoor location. Thus, the effectiveness of traditional distance-based techniques is consequently impacted by this fluctuation, especially in complex interior environments. This paper introduces two algorithms that enhance the MM algorithms to achieve higher localization accuracy, particularly for multiple targets. We highlight our contribution as follows:

1. For the first algorithm, Three Layers Bounding Box MM (TLB-MM), we focus on addressing the issue of failure in RSSI-to-distance translation. We generate the error functions by calibrating RSSI values in the specific area. These functions are then used to shape inner and outer bounding boxes. Thus, three interest boxes are formed, comprising inner, middle, and outer layers. By utilizing these interest boxes, centroids are assigned so that we can use them to decide the target location.
2. Weighted Centroid Three Layers Bounding Box MM (WC-TLB-MM) integrates TLB-MM with the WCLA for the second algorithm. By incorporating WCLA, we introduce an extra centroid into the algorithm, resulting in four centroids being utilized.
3. We expect higher localization performance by implementing the proposed algorithms, especially in scenarios involving multiple targets' localization.

The remainder of the paper is organized as follows. The related work is reviewed in Section II. Section III introduces traditional distance-based indoor localization. Our proposed algorithms, i.e., TLB-MM and WC-TLB-MM, are presented in Section IV. Sections IV and V provide the experiments, their results, and discussions. Finally, the conclusion is summarized in Section V.

II. RELATED WORK

A. RADIO FREQUENCY TECHNOLOGIES COMPARISON

Many studies have adopted distance-based techniques and Wi-Fi for indoor localization, mainly due to their ease of implementation and satisfactory performance. Several studies have indicated that Wi-Fi delivers superior accuracy to other radio frequency (RF) technologies such as Bluetooth Low

Energy (BLE), ZigBee, and LoRaWAN. In [37], the authors constructed an indoor localization system using Wi-Fi and BLE technologies. They installed three APs in an 8 m × 8 m area to localize and track the target. Wi-Fi outperformed BLE using the trilateration algorithm, with average errors of 1.3 m and 1.7 m for Wi-Fi and Bluetooth, respectively.

The work introduced in [28] uses Pycom's Lopy v1.0 hardware, which supports Wi-Fi, BLE, and LoRaWAN, to construct RSSI-based indoor localization and compare the wireless standard. To test and compare Wi-Fi, BLE, and LoRaWAN standards, they deployed the Lopy-based indoor localization system in the laboratory with a size of 8 × 8 ft^2, which contained 25 to 28 computer systems that could interfere with APs, a corridor of 23 × 23 ft^2, and a classroom of 50 × 30 ft^2 with 20 to 25 tables and chairs. The results obtained from the experiment using trilateration indicate that Wi-Fi exhibited the highest level of accuracy, with an average error of 0.54 m. LoRaWAN followed as the second most accurate option, with an average error of 0.62 m, while BLE was the least accurate, with an average error of 0.82 m.

The authors in [29] compared several radio frequency technologies, e.g., Wi-Fi, BLE, ZigBee, and LoRaWAN, based on RSSI as a parameter. They conducted a measurement campaign in two indoor environments. The first environment is a 10.8 m × 7.3 m research laboratory with some computers and several Wi-Fi and BLE devices that could cause interference. This condition allowed the research lab to represent the real-world environment. The second experiment was conducted in a smaller room without devices and contained only a table and chair. This environment represents the ideal testing area. The authors evaluated their approach in the localization accuracy and the power consumption for two environments. The results showed that Wi-Fi required a higher power consumption than other technologies. However, in terms of localization error, Wi-Fi performed better than others.

B. DISTANCE-BASED TECHNIQUES: MM AND WCLA

Trilateration is a fundamental distance-based technique that uses a geometric approach to estimate the target's position by identifying the intersection point. However, its primary limitation in practical implementation lies in accurately pinpointing this intersection point. The intersection-finding problem can result from the oversimplified assumption of various factors in the translation process, such as time-varying noise and the influence of multipath effects within the intricate surrounding environment in many practical situations [38]. This limitation motivates some researchers to apply a bounding box-based approach, the Min-Max (MM) algorithm. Instead of using an intersection point, the MM algorithm determines the target location by forming an interest box to achieve higher accuracy than the trilateration algorithm. Trilateration and MM have been compared in some studies in terms of accuracy.

The authors in [31] developed an indoor localization system based on distance measurement using a standard path loss model and RSSI. Their study evaluated and compared two fundamental distance-based techniques: trilateration and the MM algorithm. The experiments were conducted within a 5 m × 5 m area of interest, utilizing the ZigBee standard. The results indicate that the min-max algorithm outperforms trilateration in terms of accuracy, as trilateration resulted in errors of up to 3 m.

The authors in [39] developed the RSSI Filtering Method for Handling the Effects of Human Movement in an Indoor Localization System based on their understanding of RSSI, which is suspectable to the fluctuation. In a parking structure measuring 6.2 m × 3.6 m, they installed an indoor localization system using a CC2500 RF and LPC2103F microprocessor. The authors investigate how RSSI data during human movements affect the accuracy of such methods and which method shows the best position estimation result. Based on this investigation, they designed and developed a new RSSI filter to automatically reduce RSSI variation and the position estimation error caused by human movements. The results of their research indicate that without human movement, both localization methods perform similarly. However, the results also reveal that when human movement effects are present, the min-max method exhibits superior accuracy in managing the challenge of RSSI variations compared to the trilateration method.

Since the MM algorithm leverages the interest box to estimate the target location, it serves a localization with the coarse estimation regarded as the geometric centroid of the interest box. The authors in [32] introduce the improved MM with Area Partition Strategy (MM APS) to address that issue. Inspired by [40], MM APS focuses on applying the weighted centroid of the interest box. The weights eliminate some unnecessary parts of the interest box to create a smaller one. The authors assessed the performance of the proposed Min-Max-APS algorithm, and an indoor localization scenario was created using the MATLAB simulation platform. In this simulation, the measured area was represented as a 20 m × 20 m square grid with 441 evenly spaced sampling locations distributed from (0, 0) to (20, 20). The simulation shows that the localization error of MM APS can drop below 0.16 m.

The existing MM algorithms utilize the simple translation to establish a bounding box, neglecting the impact of multipath fading commonly encountered. This oversimplification can produce an error in the distance translation and decrease the localization accuracy. Thus, we propose to improve the MM algorithm by generating the error function derived from the disparity between the translated and actual distances. Integrating this function into the MM algorithm generates the three distinct circles: inner, middle, and outer circles. The middle circle is formed by translating the target's RSSI values into distances. Meanwhile, the outer and inner circles are

generated by adding and subtracting an error function from the translated distances. Using these circular regions, we create three interest boxes, yielding three potential centroids. The final estimated location is obtained by averaging the centroids. This enhancement allows for a more accurate and reliable localization process, considering the dynamic RSSI fluctuations.

Furthermore, we enhance our proposed improved MM algorithm by integrating the WCLA to increase localization accuracy. As described in [35], [41], [42], and [43], WCLA uses a different approach for estimating location than trilateration and MM. WCLA relies significantly on the RSSI-to-distance conversion to calculate the weight used to adjust all AP coordinates' centroid. This adjusted centroid is then identified as the estimated target location. By combining our enhanced MM algorithm with WCLA, we anticipate the second proposed algorithm will demonstrate excellent stability because it leverages two perspectives in RSSI-to-signal translation. We assess our proposed method by comparing it with other techniques, including the traditional MM algorithm, WCLA, and distance-free methods, i.e., the KNN-based fingerprinting technique. This thorough evaluation aims to offer valuable insights into the effectiveness and advantages of our proposed approach for indoor localization.

III. DISTANCE-BASED INDOOR LOCALIZATION

This paper focuses on developing an indoor localization system adopting an improved MM algorithm and utilizing Wi-Fi-based technology. In this section, we explore distance-based techniques, especially MM and WCLA, with advancements in translating RSSI into distances through the Log-distance path loss model.

A. LOG-DISTANCE PATH LOSS MODEL

Translating RSSI to the distance could be explained by using the path loss model, and it is a necessary step in distance-based localization techniques [11]. The log-distance path loss model is commonly used for indoor applications because it can capture the variations in signal strength affected by the multipath effect. The signal attenuation exhibits a lognormal distribution. Thus, the path loss model can be expressed as (1).

$$P_L(d) = P_L(d_0) + 10{\cdot}n{\cdot}log_{10}\left(\frac{d}{d_0}\right) + X_\sigma, \tag{1}$$

where $P_L(d)$ indicates the path loss model (in dBm) associated with the distance d. While, $P_L(d_0)$ represents the path loss at the reference distance which is typically 1 m. The path loss index in a particular environment is denoted by n. Additionally, X_σ signifies the fluctuation in measurement noise caused by shadowing within a relatively brief time frame. The RSSI is expressed by (2) as follows [44]:

$$RSSI = P_t - P_L(d). \tag{2}$$

In the formula, P_t is the signal transmission power in dBm. $A = P_t - P_L(d_0)$ represents RSSI at the reference distance 1 m. By incorporating (2) to (1), the relationship between RSSI and distance can be represented as (3)

$$RSSI = A - 10{\cdot}n \cdot log_{10}\left(\frac{d}{d_0}\right) - X_\sigma. \tag{3}$$

The multiple measured RSSI is denoted by (4)

$$\overline{RSSI} = A - 10{\cdot}n \cdot log_{10}\left(\frac{d}{d_0}\right). \tag{4}$$

Regarding (4), the distance converted from RSSI value can be obtained by (5)

$$d = d_0{\cdot}10^{\frac{A-\overline{RSSI}}{10{\cdot}n}}. \tag{5}$$

The RSSI-to-distance formula (5) is then applied in distance-based techniques. The first step of implementing the formula is recording the coordinate of APs as the anchor point. Suppose the coordinates of three APs are (x_1, y_1, z_1), (x_2, y_2, z_2), (x_3, y_3, z_3) as shown in Fig. 1. The distance-based technique is applied to determine the coordinates of the target (x_0, y_0, z_0) by employing the distance translated from RSSI values, d_1, d_2, and d_3.

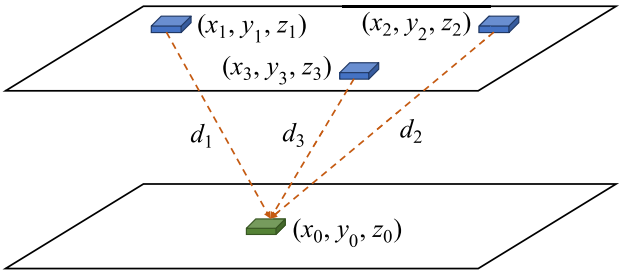

FIGURE 1. Illustration of indoor localization process using three APs.

B. MIN-MAX (MM)

In contrast to trilateration, which aims to pinpoint the precise intersection point for target estimation, MM offers an approximation by leveraging the bounding box [32] due to the challenges involved in locating the intersection point within a complicated indoor environment. MM can pinpoint the target more accurately. The imaginary bounding box is formed by adding or subtracting the AP coordinate with the distance translated from RSSI values. For simplicity, the MM algorithm with three APs is illustrated in Fig. 2. The following calculation is given by using maximum and minimum vector of formed bounding box of N APs as follows:

$$x_{\max} = \begin{bmatrix} x_1 + d_1 \\ x_2 + d_2 \\ \vdots \\ x_N + d_N \end{bmatrix}, \tag{6}$$

$$x_{\min} = \begin{bmatrix} x_1 - d_1 \\ x_2 - d_2 \\ \vdots \\ x_N - d_N \end{bmatrix}, \tag{7}$$

$$y_{\max} = \begin{bmatrix} y_1 + d_1 \\ y_2 + d_2 \\ \vdots \\ y_N + d_N \end{bmatrix}, \tag{8}$$

and

$$y_{\min} = \begin{bmatrix} y_1 - d_1 \\ y_2 - d_2 \\ \vdots \\ y_N - d_N \end{bmatrix}. \tag{9}$$

The coordinate of the target is determined by calculating the minimum value within the set of vectors $x_{\max}$ and $y_{\max}$ and the maximum value in the generated vectors $x_{\min}$ and $y_{\min}$ the mean values as follows:

$$x_{\mathrm{MM}} = \frac{\min(x_{\max}) + \max(x_{\min})}{2}, \tag{10}$$

$$y_{\mathrm{MM}} = \frac{\min(y_{\max}) + \max(y_{\min})}{2}. \tag{11}$$

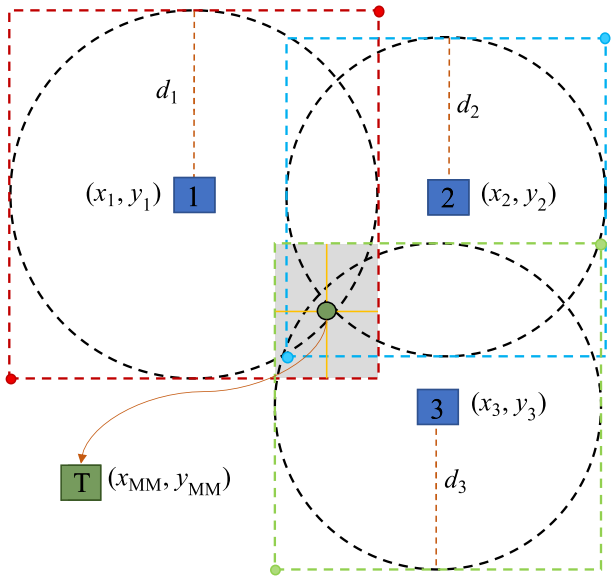

FIGURE 2. General scheme of MM with three APs.

C. WEIGHTED CENTROID LOCALIZATION ALGORITHM (WCLA)

The WCLA is an algorithm for estimating the target's location that involves shifting the centroid of the APs' locations by applying weights. This centroid is then utilized to approximate the target's location [35]. The process of shifting the centroid in WCLA is depicted in Fig. 3. The weights are obtained by inverting the distance in (5) as expressed in (12).

$$w_i = \frac{1}{d_i^g}, \tag{12}$$

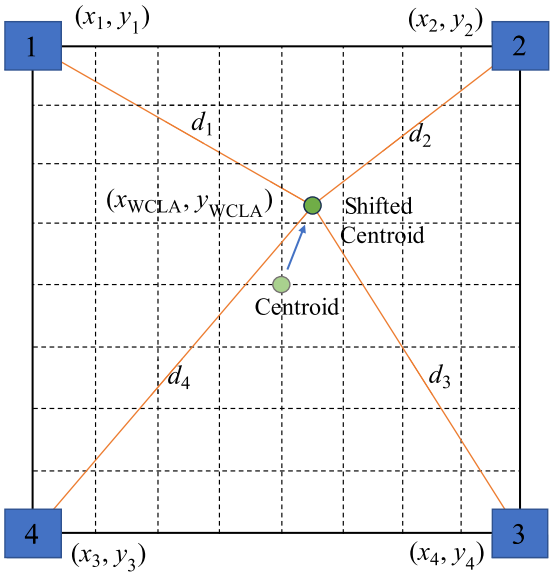

FIGURE 3. General scheme of WCLA with four APs.

where d_i is the distance converted of RSSI from AP_i, $i = 1, 2, \ldots, N$ and g is the degree of weight. Then, the final estimated position $(x_{\mathrm{WCLA}}, y_{\mathrm{WCLA}})$ is obtained by calculating the weighted centroid as follows:

$$[x_{\mathrm{WCLA}}, y_{\mathrm{WCLA}}] = \left[\frac{\sum_{i=1}^{N} w_i \cdot x_i}{\sum_{i=1}^{N} w_i}, \frac{\sum_{i=1}^{N} w_i \cdot y_i}{\sum_{i=1}^{N} w_i} \right], \tag{13}$$

where (x_i, y_i) denotes AP's location.

IV. PROPOSED IMPROVED MIN-MAX: TLB-MM AND WC-TLB-MM

This section explains two proposed improved MM algorithms to achieve higher accuracy.

A. THREE LAYERS BOUNDING BOX MM (TLB-MM)

The Three Layers Bounding Box MM (TLB-MM) algorithm improves the MM algorithm by employing the RSSI calibration process to generate error functions. Including the error function in the bounding box generation of the MM enables the creation of the inner and outer bounding boxes. In the first step, the calibration process is initiated by comparing the distances translated from the RSSI values measured at some points within the indoor environment with the theoretical RSSI values based on the path loss model. The error functions are then generated by employing polynomial regression to model the differences between the translated distances and the actual distances of the APs to calibration points (CPs) within the area of interest. The error function is mathematically expressed as follows:

$$f_{err}(d) = b_0 + a_1 \cdot d + a_2 \cdot d^2 + \ldots + a_N \cdot d^{\mathrm{k}} + \epsilon \tag{14}$$

where $f_{err}(d)$ denotes the error function based on polynomial regression model. The intercept and coefficient are represented by b_0 and a_i. k and ϵ are referred to as the degree

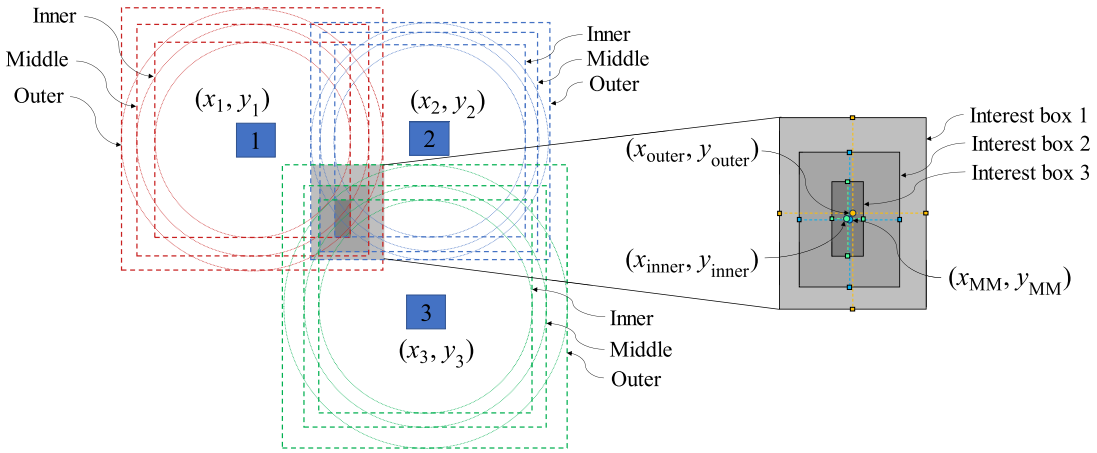

FIGURE 4. General scheme of TLB-MM with three APs.

of the polynomial and polynomial error, respectively. In the second step, the generated error function $f_{err}(d)$ is then added to (6)−(9). Thus, the inner and outer bounding boxes can be formed from (15)−(23).

$$x_{\text{min\_min}} = \begin{bmatrix} x_1 - (d_1 - f_{err}(d_1)) \\ x_2 - (d_2 - f_{err}(d_2)) \\ \vdots \\ x_N - (d_N - f_{err}(d_N)) \end{bmatrix}, \tag{15}$$

$$x_{\text{min\_max}} = \begin{bmatrix} x_1 - (d_1 + f_{err}(d_1)) \\ x_2 - (d_2 + f_{err}(d_2)) \\ \vdots \\ x_N - (d_N + f_{err}(d_N)) \end{bmatrix}, \tag{16}$$

$$y_{\text{min\_min}} = \begin{bmatrix} y_1 - (d_1 - f_{err}(d_1)) \\ y_2 - (d_2 - f_{err}(d_2)) \\ \vdots \\ y_N - (d_N - f_{err}(d_N)) \end{bmatrix}, \tag{17}$$

$$y_{\text{min\_max}} = \begin{bmatrix} y_1 - (d_1 + f_{err}(d_1)) \\ y_2 - (d_2 + f_{err}(d_2)) \\ \vdots \\ y_N - (d_N + f_{err}(d_N)) \end{bmatrix}, \tag{18}$$

$$x_{\text{max\_min}} = \begin{bmatrix} x_1 + (d_1 - f_{err}(d_1)) \\ x_2 + (d_2 - f_{err}(d_2)) \\ \vdots \\ x_N + (d_N - f_{err}(d_N)) \end{bmatrix}, \tag{19}$$

$$x_{\text{max\_max}} = \begin{bmatrix} x_1 + (d_1 + f_{err}(d_1)) \\ x_2 + (d_2 + f_{err}(d_2)) \\ \vdots \\ x_N + (d_N + f_{err}(d_N)) \end{bmatrix}, \tag{20}$$

$$y_{\text{max\_min}} = \begin{bmatrix} y_1 + (d_1 - f_{err}(d_1)) \\ y_2 + (d_2 - f_{err}(d_2)) \\ \vdots \\ y_N + (d_N - f_{err}(d_N)) \end{bmatrix}, \tag{21}$$

$$y_{\text{max\_max}} = \begin{bmatrix} y_1 + (d_1 + f_{err}(d_1)) \\ y_2 + (d_1 + f_{err}(d_1)) \\ \vdots \\ y_N + (d_1 + f_{err}(d_1)) \end{bmatrix}, \tag{22}$$

and

$$y_{\text{max\_max}} = \begin{bmatrix} y_1 + (d_1 + f_{err}(d_1)) \\ y_2 + (d_1 + f_{err}(d_1)) \\ \vdots \\ y_N + (d_1 + f_{err}(d_1)) \end{bmatrix}. \tag{23}$$

All the interest boxes in TLB-MM are formed by the overlaps of bounding boxes, as illustrated in Fig. 4. Once these interest boxes are created through the inner and outer bounding boxes, the inner and outer target locations can be estimated using (24) to (27).

$$x_{\text{inner}} = \frac{\min(x_{\text{max\_min}}) + \max(x_{\text{min\_max}})}{2}, \tag{24}$$

$$y_{\text{inner}} = \frac{\min(y_{\text{max\_min}}) + \max(y_{\text{min\_max}})}{2}, \tag{25}$$

$$x_{\text{outer}} = \frac{\min(x_{\text{max\_max}}) + \max(x_{\text{min\_min}})}{2}, \tag{26}$$

and

$$y_{\text{outer}} = \frac{\min(y_{\text{max\_max}}) + \max(y_{\text{min\_min}})}{2}. \tag{27}$$

The final target location $(x_{\text{TLB-MM}}, y_{\text{TLB-MM}})$ is estimated by

$$x_{\text{TLB-MM}} = \frac{x_{\text{inner}} + x_{\text{MM}} + x_{\text{outer}}}{3}, \tag{28}$$

and

$$y_{\text{TLB-MM}} = \frac{y_{\text{inner}} + y_{\text{MM}} + y_{\text{outer}}}{3}. \tag{29}$$

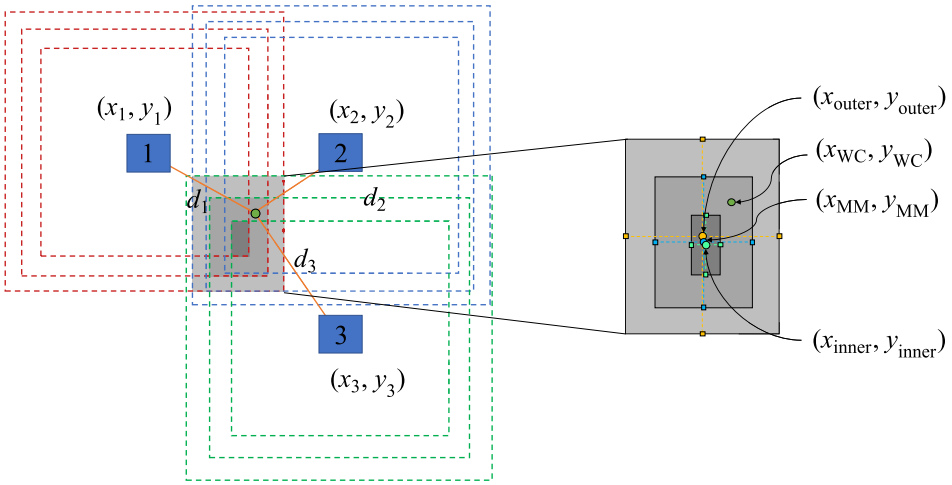

FIGURE 5. General scheme of WC-TLB-MM with three APs.

B. WEIGHTED CENTROID THREE LAYERS BOUNDING BOX MM (WC-TLB-MM)

The main idea behind the second proposed method (WC-TLB-MM) combines TLB-MM with WCLA to improve the accuracy of estimating the target's location. While the conventional MM algorithm relies on translating RSSI into distance for location estimation, WCLA utilizes the inverse conversion of distance from RSSI values as its primary approach. By integrating WCLA into TLB-MM, we harmonize two distinct perspectives on target location estimation, in which more accurate location estimation is expected. The TLB-MM process is illustrated in Fig. 5. To calculate the final coordinates, the WCLA coordinates (13) are added to (28) and (29) as follows:

$$x_{\mathrm{WC-TLB-MM}} = \frac{x_{\mathrm{TLB-MM}} + x_{\mathrm{WCLA}}}{4}, \tag{30}$$

and

$$y_{\mathrm{WC-TLB-MM}} = \frac{y_{\mathrm{TLB-MM}} + y_{\mathrm{WCLA}}}{4}. \tag{31}$$

The whole procedure of estimating location using WC-TLB-MM is described in Algorithm 1.

Algorithm 1 WC-TLB-MM Algorithm

Initialization:

1. Location of access point $AP_i (i = 1, 2, \ldots, N)$
2. Path loss exponent $n_j (j = 1, 2, \ldots, N)$
3. Value of RSSI $A_k (k = 1, 2, \ldots, N)$
4. RSSI measurements at calibration points

Procedure:

1. Calculate the translated distances $d_{translated,i} (i = 1, 2, \ldots, N)$ of RSSI measurements using (4).
2. **for** $i = 1$ **to** N **do**
3. Calculate translations error $Err = absolute(d_{actual} - d_{translated})$
4. **end for**
5. Train Polynomial Regression function $f_{err}(d)$ with the input Err and d_{actual}
6. **def** $f_{err,APl}(d)$:
7. $f_{err,APl}(d) = b_{0,APl} + a_{1,APl} \cdot d + a_{2,APl} \cdot d^2 + \ldots +$
8. $a_{N,APl} \cdot d^{\mathrm{k}} + \epsilon, (l = 1, 2, \ldots, M)$
9. **return** Err_{APl}
10. Create interest boxes using (6) − (9) and (15) − (23)
11. Estimate the target location by TLB-MM
12. Calculate w_i using (13)
13. Estimate the WC-TLB-MM location by (30) and (31)

V. EXPERIMENT

We evaluate the performance of our proposed TLB-MM and WC-TLB-MM and compare them with other traditional distance-based algorithms.

A. MEASUREMENT LAYOUT

The selected study environment is a laboratory with a vinyl floor and various interior elements such as tables, chairs, and robotic arms. These elements could obstruct the signal propagation from the APs to the target. The accuracy of indoor localization is usually enhanced when more APs are employed. However, it also increases the complexity and hardware deployment costs. Our experiment utilized three APs, the minimum requirement for the traditional distance-based technique. The APs were placed in the corner of a 10.17 m × 9.12 m designed environment. The actual environment and the measurement layout are illustrated in Fig. 6 and Fig. 7, respectively.

B. RSSI-BASED INDOOR LOCALIZATION SYSTEM

1) HARDWARE AND SOFTWARE

The data collection system primarily employed the ESPino32 module, which is equipped with the ESP32 chip and supports

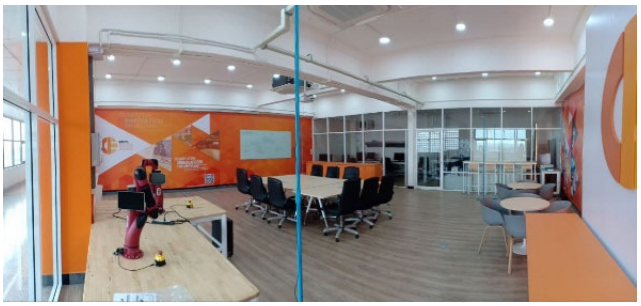

FIGURE 6. Selected environment (laboratory).

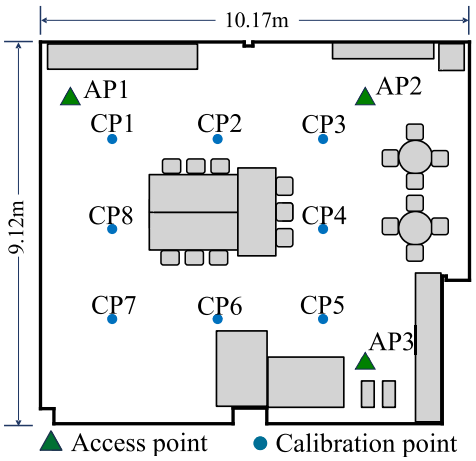

FIGURE 7. Measurement layout with calibration points.

FIGURE 8. ESPino32 Wi-Fi/BLE module.

both Wi-Fi and BLE standards. Fig. 8 depicts an ESPino32 module. We configured this module to serve as Wi-Fi access points (APs) and as the targets or receivers using the Arduino IDE. To assess the performance of our proposed algorithm, we processed the RSSI data using Python 3.9.7 64-bit. Table 1 presents the details of the hardware and software setup.

To confirm the effectiveness of the ESPino32 module, we carried out RSSI measurements in an outdoor setting that mimicked conditions resembling an open space free from obstructions. These measurements involved recording RSSI

TABLE 1. Specification of hardware and software used in this work.

Function	Items	Description
Wi-Fi hardware	ESPino32 module	- Protocol: 802.11b/g/n 2.4 GHz - Working voltage/current: 2.3-3.6 V/80 mA - Dimension: 25.4 mm × 65 mm
Power supply	Power bank	- 10000 mAh
Data processing	Python	- version 3.9.7 64-bit
Database	Firebase	- Cloud database (free license)
Central processing unit	Computer	- Processor: AMD Ryzen 9 3900X 12-Core - RAM: 32 GB - Operating system: 64-bit

values at distances ranging from 0 to 5 m between the transmitter and receiver, resulting in 31 RSSI at each measurement point. Fig. 9 illustrates the path loss model outcomes for all the modules under these ideal environmental conditions.

2) DATA ACQUISITION SYSTEM

In this work, we set up an IoT data acquisition system employing Wi-Fi devices. The system aims to localize one or more targets utilizing a star topology. The data acquisition procedure commences by programming the APs to transmit RSSI signals. Subsequently, the target devices collect RSSI values from three APs and send this data to a cloud database. All the received RSSI signals are stored in this cloud database, relayed, and made accessible on a computer, which functions as the central processing unit. Fig. 10 illustrates the structure of this data acquisition system.

TABLE 2. Path loss parameters related to all APs in selected environment.

Parameter	AP 1	AP 2	AP 3
n	1.55	2.27	3.04
A (dBm)	-39.59	-33.02	-26.49

C. EVALUATION PROCEDURE

The first step in the experiment was to estimate the path loss exponent n and A value used in (5). We conducted RSSI measurements to estimate these parameters at eight designated CPs depicted in Fig. 8. These measurements allowed us to estimate the values of n and A for each access point (AP) using the least squares method [45]. Table 2 presents the path loss parameters for the selected environment.

To assess the performance of the proposed algorithms, we conducted four different scenarios involving varying the number of targets and considering dynamic and static movements, simulating the localization process for multiple targets and their movement patterns as depicted in Fig. 11. In Scenario 1, a single target moved in clockwise and

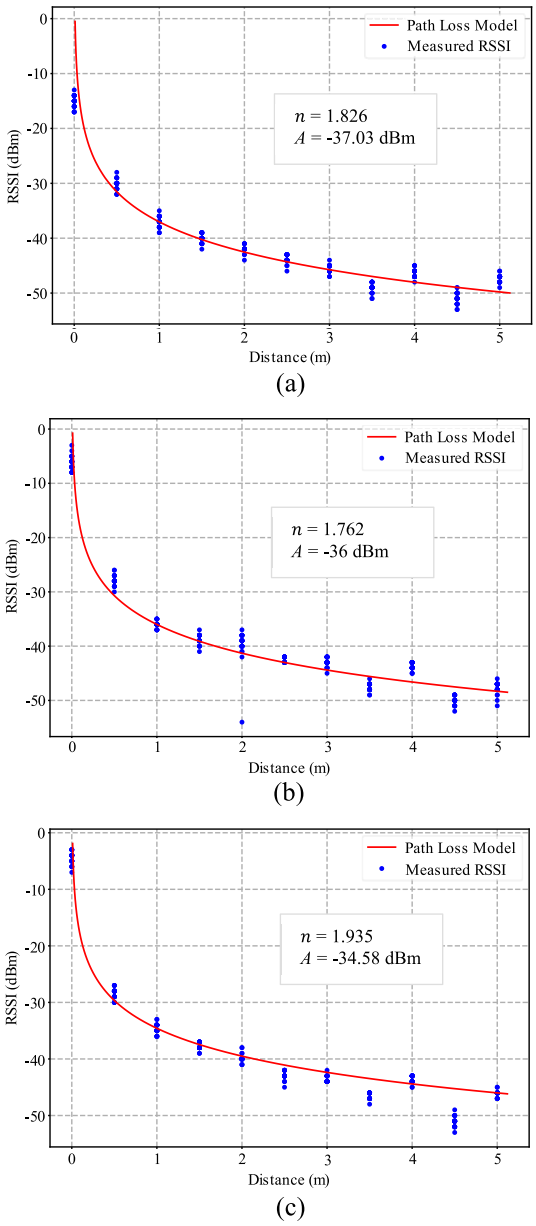

FIGURE 9. Path loss measurement in outdoors: (a) AP1 (b) AP2 (c) AP3.

counterclockwise directions. Throughout this scenario, we collected RSSI data at regular intervals across 36 specific points, with each point recording RSSI values ranging from 10 to 14 data, corresponding to the clockwise and counterclockwise movements. In scenario 2, while Target *T1* moved in a clockwise direction, Target *T2* moved counterclockwise, and vice versa. Similar to Scenario 1, in Scenario 2, we recorded RSSI data at 36 distinct points for each target and each direction. For Scenario 3, we evaluated the localization of target *T1* as a static target and *T2* as a dynamic target. The dynamic target followed a predetermined path, and we strategically positioned it at 12 points near the access points (APs) and corners that could influence the estimation of the static target. The static target in this scenario represented a person seated in a chair. Scenario 4 explored three conditions with static targets: A, B, and C. In condition A, target *T1* was seated in a chair, and the receiver device was placed on a table nearby to evaluate the effect of human body obstruction. In condition B, targets *T1* and *T2* were simulated to sit adjacent to each other, and the receiver devices were placed on the desk in front of them. In condition C, two receiver devices were placed on the desk without any people present, allowing us to compare it with condition B, with and without human presence.

D. EVALUATION METRICS

After obtaining the estimated location using the proposed algorithms, we assess the accuracy of these localization results and measure this efficiency. Accuracy is determined by measuring the distance error in meters (m) and its cumulative distribution functions (CDFs). At the same time, the computing time of algorithms was used to assess their efficiency. Suppose there are some recorded target locations; we utilized mean localization error (MLE) that calculates the distance between the actual position $(x_{\text{act}}, y_{\text{act}})$ and the estimated position as the error $(x_{\text{est}}, y_{\text{est}})$. If the position of the target as $i = 1, 2, 3, \ldots, L$, the MLE can be expressed as

$$MLE = \frac{1}{L}\sum_{i=1}^{L}\sqrt{(x_{\text{act},i} - x_{\text{est},i})^2 + (y_{\text{act},i} - y_{\text{est},i})^2}. \quad (32)$$

VI. RESULTS AND DISCUSSION

This section presents the results and analysis of the proposed localization algorithms by comparing them to traditional distance-based algorithms, i.e., TRI, MM, and WCLA, and the fingerprint technique employing K-Nearest Neighbors (KNN).

TABLE 3. Polynomial regression parameters related to all APs.

Parameter	AP 1	AP 2	AP 3
b_0	-2.674	-0.525	1.660
a_1	2.455	0.617	-0.549
a_2	-0.219	0.014	0.097

A. RSSI CALIBRATION

An essential aspect of our proposed algorithms involves determining the optimal degree of the polynomial regression. We conducted tests using polynomial regressions with degrees ranging from 1 to 5 to identify the optimal degree. This polynomial regression fitting was carried out in scenario 1 (benchmark). The results, as illustrated in Fig. 12, clearly indicate that the optimal degree of the polynomial is 2. Table 3 shows the parameters of the polynomial regression used in this paper.

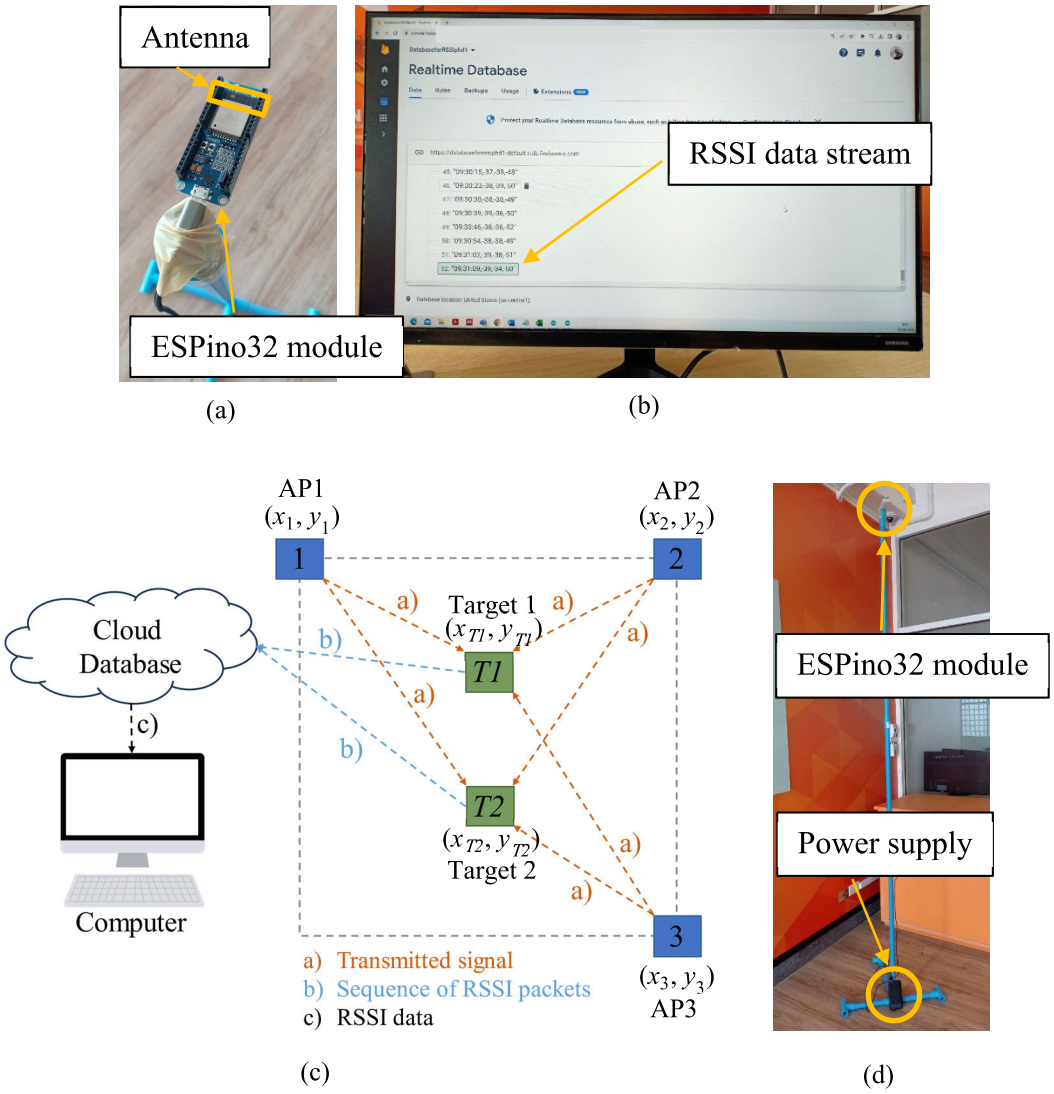

FIGURE 10. RSSI acquisition system: (a) receiver/target (b) monitoring system (c) scheme of indoor localization system with two targets (d) AP.

B. LOCATION ESTIMATION RESULTS

We considered the localization test under four scenarios, i.e., scenarios 1, 2, 3, and 4. The performance of TLB-MM and WC-TLB-MM are evaluated concerning mean localization error (MLE) and detailed with cumulative distribution function (CDF). The comparison of MLE and CDF of proposed algorithms and other traditional distance-based techniques for scenarios 1, 2, and 3 are depicted in Fig. 13 and Fig. 14. Meanwhile, the MLE of scenario 4 is presented in Table 4. In scenario 1, WC-TLB-MM demonstrated superior performance to other techniques, achieving an accuracy of 2.1317 m with 47.22% of the localization errors falling within 2 m. The next highest accuracy was TLB-MM, with an overall error of 2.1577 m, and 45.83% of the localization errors were below 2 m. WCLA achieved slightly lower accuracy than TLB-MM, with MLE of 2.2244 m and approximately 51.39% of localization errors below 2 m. MM has an MLE of 2.5505 m, with 34.72% of localization errors below 2 m. In scenario 2, we simulate two persons that move in opposite directions. For the target *T1*, TLB-MM demonstrated to be the best algorithm with an error of 1.9835 m with 56.94% of localization errors below 2 m, and WC-TLB-MM followed with an error of 2.0772 m with 58.33% of errors within 2 m. Following closely behind WC-TLB-MM, in third and fourth, were WCLA and MM, resulting in an overall error of 2.1466 m with 55.55% of errors below 2 m and 2.3457 m with 48.61% below 2 m, respectively. In contrast to the location estimation of target *T1*, WC-TLB-MM yielded the highest accuracy compared to others in estimating the location of target *T2*. It has an MLE of 2.2832 m with 44.44% errors below 2 m. This result is higher than WCLA and TLB-MM in the second and third best algorithms with the MLE of

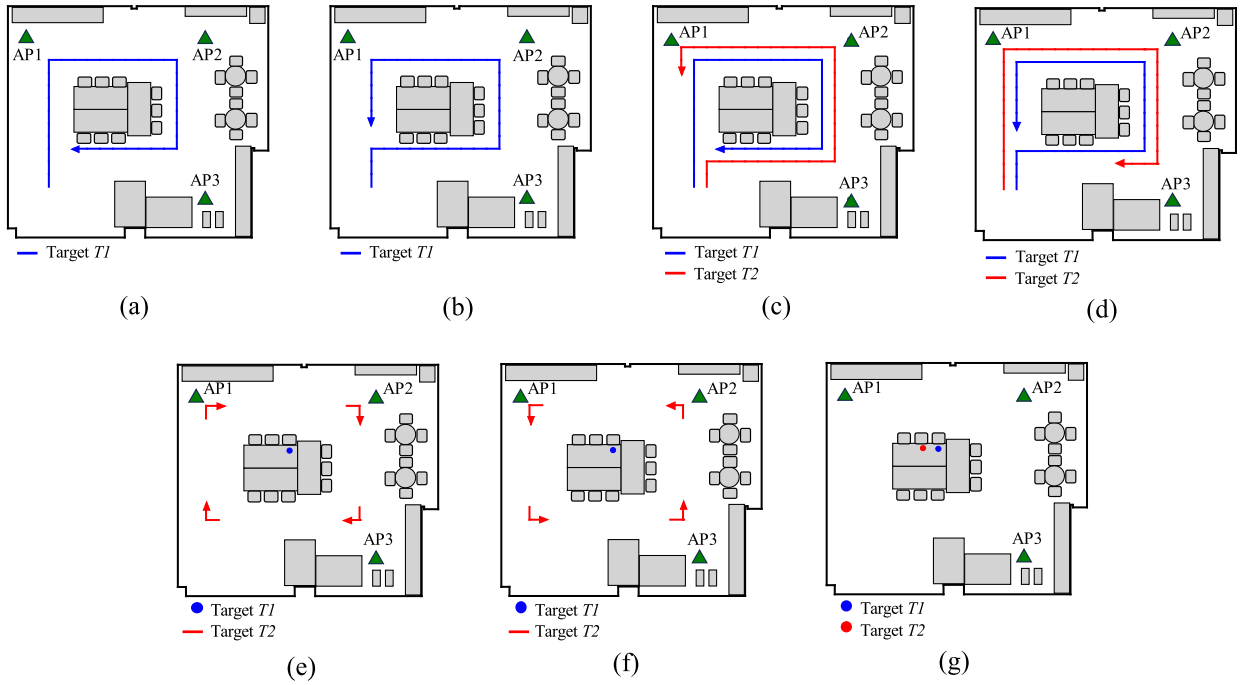

FIGURE 11. Target movement scenarios: (a) Scenario 1 clockwise (b) Scenario 1 counterclockwise (c) Scenario 2 target 1 clockwise (d) Scenario 2 target 1 counterclockwise (e) Scenario 3 target 2 clockwise (f) Scenario 3 target 2 counterclockwise and (g) Scenario 4 static targets.

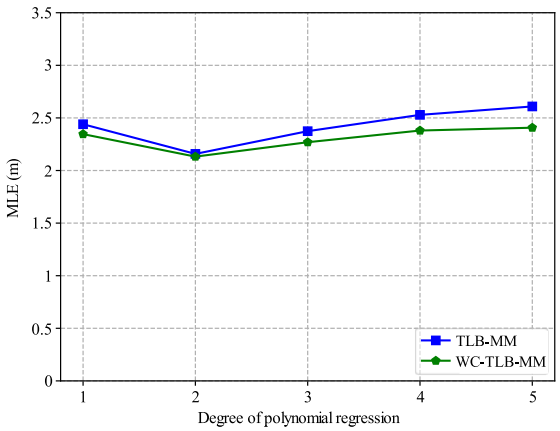

FIGURE 12. Degree of polynomial regression comparison in scenario 1.

2.3087 m and 2.3425 m, respectively. In that MLE, 43.06% errors of WCLA and TLB-MM are below 2 m. The last, MM has the MLE of 2.3826 m with 41.67% errors are below 2 m.

Like Scenario 2, we conducted an indoor localization process for two targets in Scenario 3. However, in this scenario, target *T1* remained seated in a chair instead of both targets moving, while target *T2* exhibited dynamic movement. Regarding target *T2*, we focused on several points close to the corner and the APs to evaluate the localization results when a human body possibly obstructed the signal. In the localization of target *T1*, TLB-MM emerged as the superior algorithm, achieving the lowest MLE of 1.3845 m, with approximately 95.83% of errors falling within 2 m. The following most accurate algorithm was WC-TLB-MM, which yielded an MLE of 1.8493 m, with around 70.83% of errors below 2 m. WCLA and MM followed closely, with MLEs of 2.0025 m and 3.1308 m and 50% and 4% of errors below 2 m, respectively. For target *T2*, the localization results were slightly different. The proposed algorithms exhibited similar accuracy to the MM algorithm, with MLEs approximately 6.66%, 5.19%, and 4.58% lower than WCLA.

In Scenario 4, we established a fixed target placement scenario with only one person seated on the chair for Condition A. TLB-MM demonstrated the highest accuracy, with an error of 1.463 m. The second-best algorithm, WCLA, exhibited slightly lower accuracy than TLB-MM, with an error of 1.465 m. Meanwhile, WC-TLB-MM and MM had errors of approximately 1.657 m and 2.082 m, respectively.

In Condition B, the proposed TLB-MM and WC-TLB-MM algorithms yielded the lowest error, 0.756 m and 1.204 m, respectively. However, MM and WCLA performed less effectively than Condition A due to signal obstruction by human Target T2. MM had an error of 2.313 m, while WCLA had an error of 1.491 m.

For Condition C, where there was no human presence, all algorithms provided higher accuracy than the other conditions. TLB-MM, WC-TLB-MM, and MM achieved approximately twice the accuracy of the error results in Condition B. Although WCLA did not perform as well as the others, it still offered higher accuracy than Condition B.

C. PROPOSED ALGORITHMS VS. FINGERPRINT

Many studies have highlighted the superior performance of the fingerprint technique over distance-based techniques,

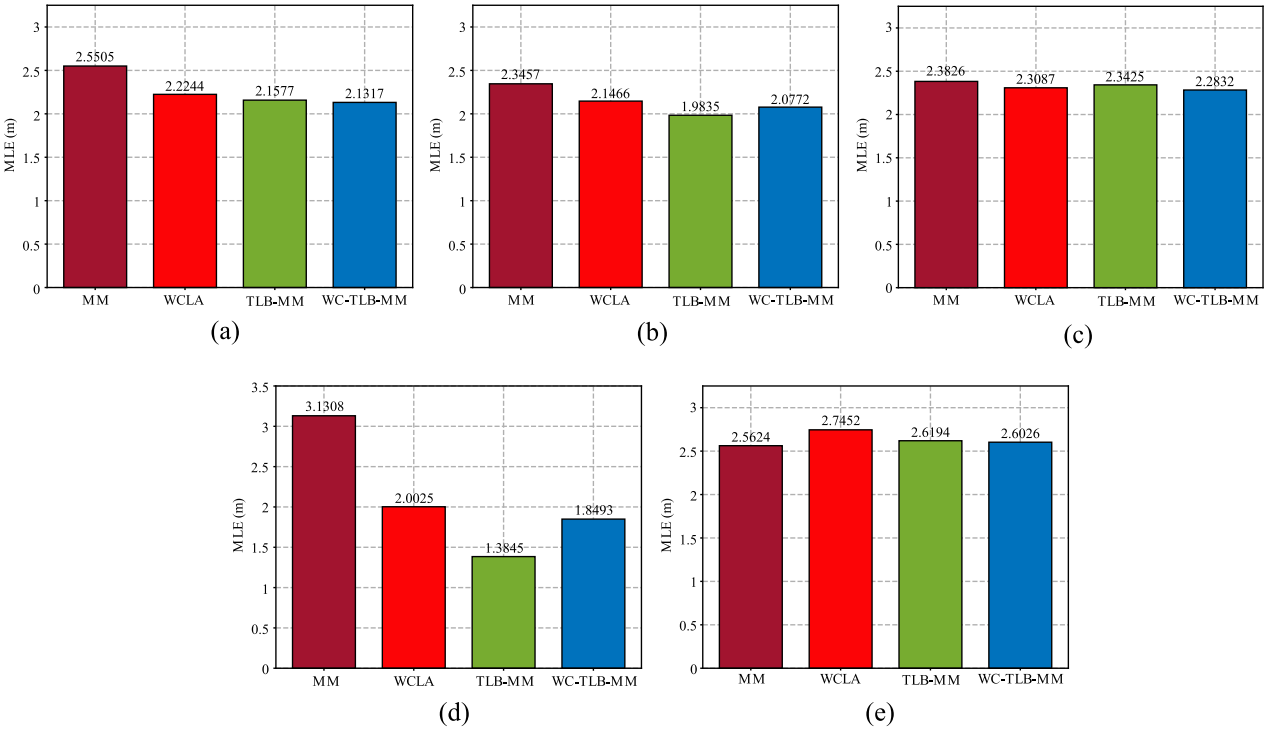

FIGURE 13. MLE comparison: (a) Scenario 1 (b) Scenario 2 target 1 (c) Scenario 2 target 2 (d) Scenario 3 target 1 and (e) Scenario 3 target 2.

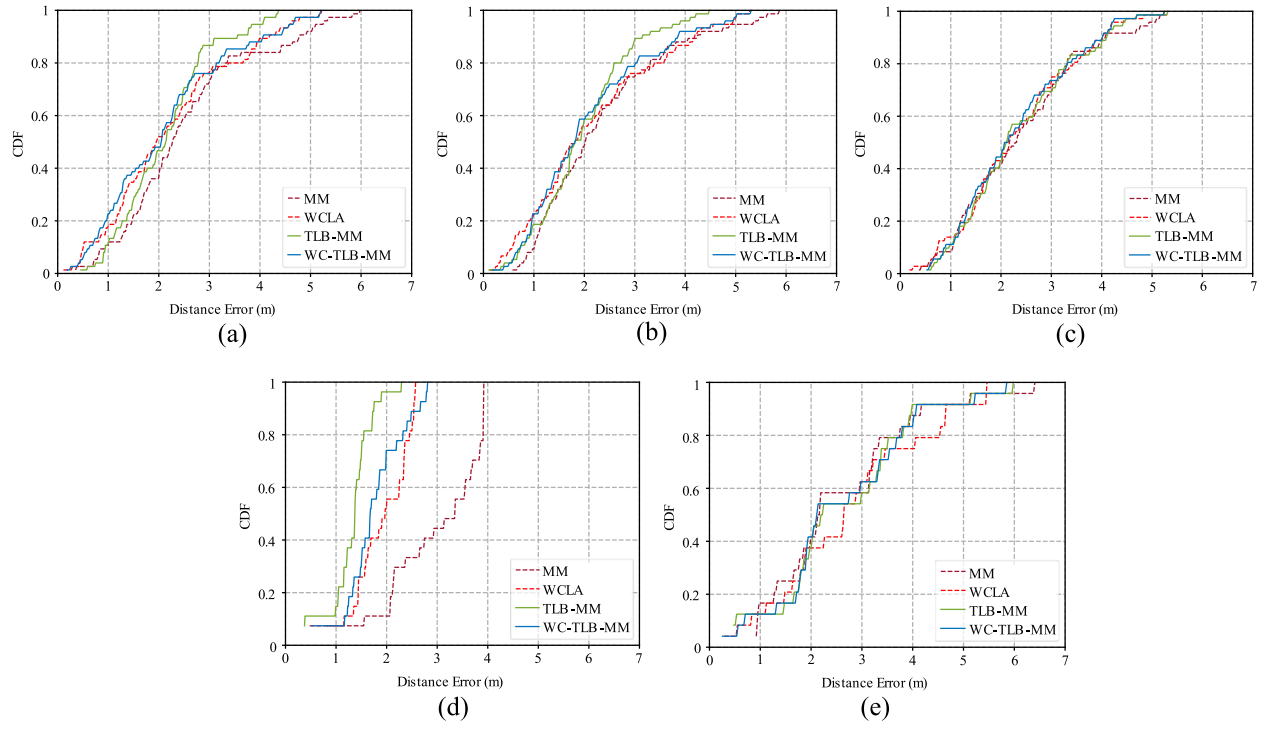

FIGURE 14. CDF comparison: (a) Scenario 1 (b) Scenario 2 target 1 (c) Scenario 2 target 2 (d) Scenario 3 target 1 and (e) Scenario 3 target 2.

particularly in complex indoor environments with a high density of interior objects and furniture. However, it is worth noting that the fingerprint technique is susceptible to rapid environmental changes, such as the presence of multiple targets. To further evaluate our proposed algorithms, we compared them to the fingerprint technique. As illustrated in Fig. 16, the fingerprint database was created by storing RSSI values collected at uniformly distributed reference points

TABLE 4. Localization results of scenario 4.

Target	Conditions	Localization errors (m)			
		MM	WCLA	TLB-MM	WC-TLB-MM
T1	A	2.082	1.465	1.463	1.657
	B	2.313	1.491	0.756	1.204
	C	1.277	1.284	0.314	0.538

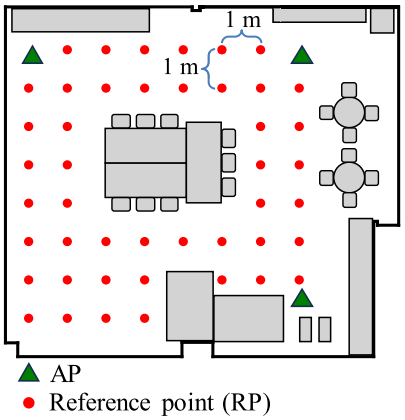

FIGURE 15. Fingerprint database construction map.

(RPs) with a 1 m grid density. Several works have employed the K-Nearest Neighbors (KNN) pattern-matching algorithm in the fingerprint technique. Consequently, we chose the KNN as the benchmark algorithm for fingerprinting. With our measurement data, we investigated the K values ranging from 1 to 20 to determine the opimal K value and found that the K of 1 gave the best result. The compared results from our proposed algorithms and the fingerprint technique are presented in Fig. 15.

In scenario 1, the fingerprint technique performs better than both TLB-MM and WC-TLB-MM in accurately determining the location of target T1. The fingerprint technique achieves an error of 2.0992 m, while TLB-MM and WC-TLB-MM exhibit errors of 2.79% and 1.55% higher than the fingerprint technique. However, the situation changes in scenarios 2 and 3 due to the presence of multiple individuals. In these scenarios, TLB-MM and WC-TLB-MM demonstrate superior accuracy compared to the fingerprint technique for localizing target T1. In scenario 2, TLB-MM and WC-TLB-MM have significantly lower errors in localizing target T1 compared to the fingerprint technique, which has an error of 2.6882 m. Our proposed algorithms achieve 26.22% and 22.73% lower error than the fingerprint technique, respectively. In scenario 3, the fingerprint technique estimates the location of target T1 with an error of 3.5481 m, while TLB-MM and WC-TLB-MM exhibit higher accuracy, with errors that are 60.98% and 47.88% lower than the fingerprint technique, respectively. For target T2 in scenarios 2 and 3, WC-TLB-MM shows larger differences in errors compared to TLB-MM when compared to the fingerprinting technique. In scenario 2, WC-TLB-MM and TLB-MM enhance accuracy by 19.6% and 17.51%, respectively, compared to the fingerprinting technique. In scenario 3, both WC-TLB-MM and TLB-MM improve accuracy with a decreased error of 19.4% and 16.72%, respectively, relative to the fingerprint technique.

TABLE 5. Comparison results of proposed algorithms vs. fingerprint technique for scenario 4.

Target	Conditions	Localization errors (m)		
		KNN	TLB-MM	WC-TLB-MM
T1	A	6.049	1.463	1.657
	B	3.255	0.756	1.204
	C	1.287	0.314	0.538

TABLE 6. Localization running time comparison.

Algorithms	Running Time in millisecond (ms)			
	Scenario			
	1	2	3	4
MM	0.273	0.459	0.447	0.238
WCLA	0.207	0.363	0.345	0.205
TLB-MM	0.479	0.559	0.552	0.455
WC-TLB-MM	0.505	0.657	0.622	0.523
KNN	0.853	1.438	1.378	0.851

In Scenario 4, we compared the accuracy of our proposed algorithms with the fingerprint technique, and the results are presented in Table 5. Based on the table, our proposed algorithms outperform the fingerprint technique. For Condition A, TLB-MM achieved a 75.81% lower error than the fingerprint technique, which had an error of 6.049 m. WC-TLB-MM also demonstrated superior performance with a 72.61% lower error than the fingerprint technique. In Condition B, the fingerprint technique resulted in an error of 3.255 m. At the same time, TLB-MM and WC-TLB-MM exhibited significantly better performance, with errors that were 76.77% and 63.01% lower than the fingerprint technique, respectively. Finally, in Condition C, TLB-MM achieved an error approximately

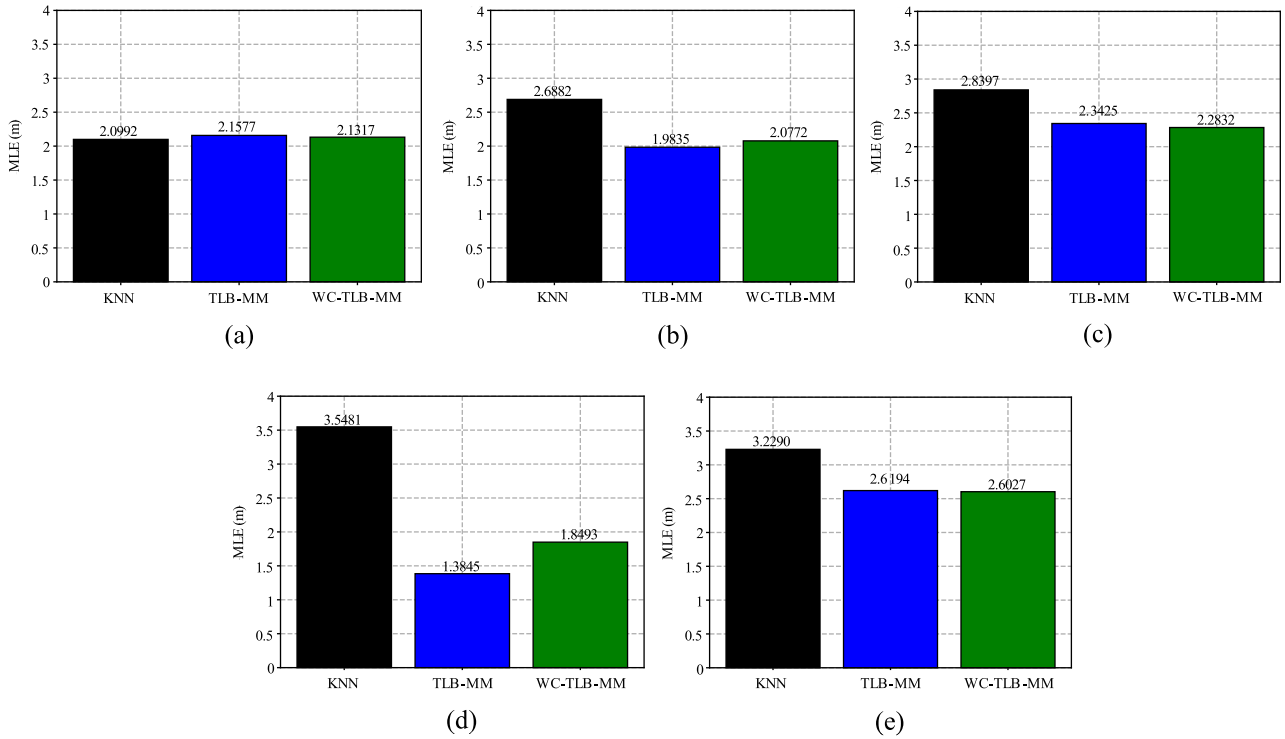

FIGURE 16. MLE comparison of proposed algorithms with fingerprint technique: (a) Scenario 1 (b) Scenario 2 target 1 (c) Scenario 2 target 2 (d) Scenario 3 target 1 and (e) Scenario 3 target 2.

75.6% lower than the fingerprint technique, while WC-TLB-MM demonstrated a 58.2% lower error.

D. INVESTIGATION OF COMPUTATIONAL TIME AND MEMORY USAGE

In order to assess the efficiency of the proposed TLB-MM and WC-TLB-MM, we also consider the computational time and memory usage. This efficiency is evaluated and compared to other related algorithms, namely MM, WCLA, and the KNN fingerprint technique. Table 6 outlines the comparison of localization computational time, while Table 7 presents the comparison of memory usage for each algorithm. As distance-based techniques represent a direct localization approach, we only consider the online phase of the KNN fingerprint technique in this comparison across all scenarios. Scenario 4 is exclusively represented by Condition A, as all conditions are identical in terms of computation. Based on computational time and memory usage, our proposed algorithms exhibit higher values compared to traditional MM and WCLA. However, they can perform better than KNN. Finally, when considering both accuracy and efficiency, our proposed algorithms are still preferable.

TABLE 7. Comparison of memory usage in algorithms.

Algorithms	Memory Usage in mebibyte (MiB)			
	Scenario			
	1	2	3	4
MM	155.78	156.32	157.87	156.34
WCLA	155.49	155.82	156.14	155.66
TLB-MM	207.84	208.77	209.04	208.87
WC-TLB-MM	208.19	208.84	208.9	208.89
KNN	209.08	210.04	209.93	209.91

E. DISCUSSION

The experimental results revealed valuable insights into the practical application of TLB-MM and WC-TLB-MM. Regarding accuracy, in scenario 1, our proposed algorithms demonstrate reduced errors compared to traditional distance-based techniques. Although our algorithms have slightly lower accuracy than the fingerprint technique, they offer greater flexibility in localizing objects in rapidly changing environments. It is well-known that the fingerprinting technique outperforms distance-based methods in less dynamic environments. Furthermore, our proposed algorithms are more efficient than the fingerprint technique regarding computational time.

In other scenarios, our proposed algorithms have significantly lower accuracy than the fingerprint technique. In scenarios 2 and 3, TLB-MM is superior in localizing target *T1*, delivering the highest level of accuracy compared to other algorithms. This proposed algorithm consistently achieves remarkable accuracy levels. Following closely in accuracy is our second proposed algorithm, i.e., WC-TLB-MM. However, when estimating the position of target *T2*, the proposed

WC-TLB-MM exhibits the highest accuracy. At the same time, the TLB-MM has similar results with MM and WCLA.

The results of the localization error in conditions B and C reveal that in scenario 4, our proposed algorithms provide highly improved accuracy. Moreover, considering the results of static target localization in both conditions B and C, it becomes evident that the presence of humans has a more significant influence than signal interference from another target. In conclusion, our proposed algorithms can consistently provide the highest accuracy for localizing static targets, with TLB-MM being the top-performing algorithm, followed by WC-TLB-MM.

VII. CONCLUSION

In this paper, we develop the RSSI-based indoor localization system and extend the traditional MM algorithm, i.e., TLB-MM and WC-TLB-MM, to achieve a higher localization accuracy. The RSSI calibration process is performed in the proposed TLB-MM to generate the distance error functions. These functions compensate for the multipath fading in the complex indoor environment. Three bunding boxes, i.e., inner, middle, and outer, are generated by integrating the functions into the MM algorithm. The target location is obtained by averaging the estimated location from the inner, middle, and outer bounding boxes. The proposed WC-TLB-MM algorithm estimates the location based on a combination of TLB-MM and WCLA.

Experiments using the Wi-Fi, 2.4 GHz, IEEE 802.11 wireless sensor network in the laboratory with four scenarios have been tested to evaluate the proposed algorithms. Scenario 1 simulates a person who brought the target device and moved around. In scenario 2, two people who brought the devices move in opposite directions. In scenario 3, one person was mobile while another remained seated in a chair. Lastly, in Scenario 4, both persons were seated, and the target devices were positioned on the table in front of them. The results from our experiments demonstrate that the proposed algorithms outperform the traditional distance-based method in terms of accuracy. TLB-MM exhibits the slightest error in estimating the location of target *T1* in all scenarios. Meanwhile, WC-TLB-MM consistently yields lower errors for all targets in every scenario. In comparison to the KNN fingerprint technique, both TLB-MM and WC-TLB-MM demonstrated enhanced capabilities in localizing multiple targets. Furthermore, considering computational time and memory usage, our proposed algorithms (TLB-MM and WC-TLB-MM) emerge as preferable options with satisfactory results.

Our forthcoming research will investigate and explore the challenges of RSSI utilization in indoor localization. This comprehensive exploration will encompass the impact of multipath fading on distance-based and fingerprint-based localization methods, focusing on strategies to enhance accuracy by mitigating the multipath effect. Additionally, the insights gained from this study will be implemented in various simulations designed to mimic real-world scenarios closely.

ACKNOWLEDGMENT

The authors would like to thank Thoriq Tri Prabowo for assistance with measurements.

REFERENCES

[1] F. Furfari, A. Crivello, P. Baronti, P. Barsocchi, M. Girolami, F. Palumbo, D. Quezada-Gaibor, G. M. M. Silva, and J. Torres-Sospedra, "Discovering location based services: A unified approach for heterogeneous indoor localization systems," *Internet Things*, vol. 13, Mar. 2021, Art. no. 100334, doi: 10.1016/j.iot.2020.100334.

[2] J. Zhang, G. Han, N. Sun, and L. Shu, "Path-loss-based fingerprint localization approach for location-based services in indoor environments," *IEEE Access*, vol. 5, pp. 13756–13769, 2017, doi: 10.1109/ACCESS.2017.2728789.

[3] V. Moghtadaiee, S. A. Ghorashi, and M. Ghavami, "New reconstructed database for cost reduction in indoor fingerprinting localization," *IEEE Access*, vol. 7, pp. 104462–104477, 2019, doi: 10.1109/ACCESS.2019.2932024.

[4] P. S. Farahsari, A. Farahzadi, J. Rezazadeh, and A. Bagheri, "A survey on indoor positioning systems for IoT-based applications," *IEEE Internet Things J.*, vol. 9, no. 10, pp. 7680–7699, May 2022, doi: 10.1109/JIOT.2022.3149048.

[5] W. C. S. S. Simões, G. S. Machado, A. M. A. Sales, M. M. de Lucena, N. Jazdi, and V. F. de Lucena, "A review of technologies and techniques for indoor navigation systems for the visually impaired," *Sensors*, vol. 20, no. 14, p. 3935, Jul. 2020, doi: 10.3390/s20143935.

[6] P. Roy and C. Chowdhury, "A survey of machine learning techniques for indoor localization and navigation systems," *J. Intell. Robotic Syst.*, vol. 101, no. 3, Mar. 2021, doi: 10.1007/s10846-021-01327-z.

[7] S. J. Hayward, K. van Lopik, C. Hinde, and A. A. West, "A survey of indoor location technologies, techniques and applications in industry," *Internet Things*, vol. 20, Nov. 2022, Art. no. 100608, doi: 10.1016/j.iot.2022.100608.

[8] H. Liu, H. Darabi, P. Banerjee, and J. Liu, "Survey of wireless indoor positioning techniques and systems," *IEEE Trans. Syst., Man Cybern., C Appl. Rev.*, vol. 37, no. 6, pp. 1067–1080, Nov. 2007, doi: 10.1109/tsmcc.2007.905750.

[9] J. Wichmann, "Indoor positioning systems in hospitals: A scoping review," *Digit. Health*, vol. 8, Jan. 2022, Art. no. 205520762210816, doi: 10.1177/20552076221081696.

[10] A. Yassin, Y. Nasser, M. Awad, A. Al-Dubai, R. Liu, C. Yuen, R. Raulefs, and E. Aboutanios, "Recent advances in indoor localization: A survey on theoretical approaches and applications," *IEEE Commun. Surveys Tuts.*, vol. 19, no. 2, pp. 1327–1346, 2nd Quart., 2017, doi: 10.1109/COMST.2016.2632427.

[11] B. Yang, L. Guo, R. Guo, M. Zhao, and T. Zhao, "A novel trilateration algorithm for RSSI-based indoor localization," *IEEE Sensors J.*, vol. 20, no. 14, pp. 8164–8172, Jul. 2020, doi: 10.1109/jsen.2020.2980966.

[12] X. Zhang, Y. Zhang, G. Liu, and T. Jiang, "AutoLoc: Toward ubiquitous AoA-based indoor localization using commodity WiFi," *IEEE Trans. Veh. Technol.*, vol. 72, no. 6, pp. 8049–8060, Jun. 2023, doi: 10.1109/TVT.2023.3243912.

[13] W. Xiong, C. Schindelhauer, H. C. So, and S. J. Rupitsch, "A message passing based iterative algorithm for robust TOA positioning in impulsive noise," *IEEE Trans. Veh. Technol.*, vol. 72, no. 1, pp. 1048–1057, Jan. 2023, doi: 10.1109/TVT.2022.3203487.

[14] W. Zhao, A. Goudar, and A. P. Schoellig, "Finding the right place: Sensor placement for UWB time difference of arrival localization in cluttered indoor environments," *IEEE Robot. Autom. Lett.*, vol. 7, no. 3, pp. 6075–6082, Jul. 2022, doi: 10.1109/LRA.2022.3165181.

[15] A. Nessa, B. Adhikari, F. Hussain, and X. N. Fernando, "A survey of machine learning for indoor positioning," *IEEE Access*, vol. 8, pp. 214945–214965, 2020, doi: 10.1109/ACCESS.2020.3039271.

[16] D. J. Suroso, F. Y. M. Adiyatma, P. Cherntanomwong, and P. Sooraksa, "Fingerprint database enhancement by applying interpolation and regression techniques for IoT-based indoor localization," *Emerg. Sci. J.*, vol. 4, pp. 167–189, Jan. 2022, doi: 10.28991/esj-2021-sp1-012.

[17] B. Yang, Q. Qiu, Q.-L. Han, and F. Yang, "Received signal strength indicator-based indoor localization using distributed set-membership filtering," *IEEE Trans. Cybern.*, vol. 52, no. 2, pp. 727–737, Feb. 2022, doi: 10.1109/TCYB.2020.2983544.

[18] D. J. Suroso, P. Cherntanomwong, and P. Sooraksa, "Indoor device-free localization using received signal strength indicator and illuminance sensor for random-forest-based fingerprint technique," *Sensors Mater.*, vol. 33, no. 12, pp. 4331–4345, 2021, doi: 10.18494/SAM.2021.3421.
[19] H. Zhang, Z. Wang, W. Xia, Y. Ni, and H. Zhao, "Weighted adaptive KNN algorithm with historical information fusion for fingerprint positioning," *IEEE Wireless Commun. Lett.*, vol. 11, no. 5, pp. 1002–1006, May 2022, doi: 10.1109/LWC.2022.3152610.
[20] G. Chen, X. Guo, K. Liu, X. Li, and J. Yang, "RWKNN: A modified WKNN algorithm specific for the indoor localization problem," *IEEE Sensors J.*, vol. 22, no. 7, pp. 7258–7266, Apr. 2022, doi: 10.1109/JSEN.2022.3155902.
[21] A. Chriki, H. Touati, and H. Snoussi, "SVM-based indoor localization in wireless sensor networks," in *Proc. 13th Int. Wireless Commun. Mobile Comput. Conf. (IWCMC)*, Jun. 2017, pp. 1144–1149, doi: 10.1109/IWCMC.2017.7986446.
[22] H. A. Abbas, N. W. Boskany, K. Z. Ghafoor, and D. B. Rawat, "Wi-Fi based accurate indoor localization system using SVM and LSTM algorithms," in *Proc. IEEE 22nd Int. Conf. Inf. Reuse Integr. Data Sci. (IRI)*, Aug. 2021, pp. 416–422, doi: 10.1109/IRI51335.2021.00065.
[23] D. Sun, E. Wei, L. Yang, and S. Xu, "Improving fingerprint indoor localization using convolutional neural networks," *IEEE Access*, vol. 8, pp. 193396–193411, 2020, doi: 10.1109/ACCESS.2020.3033312.
[24] J. Song, M. Patel, and M. Ghaffari, "Fusing convolutional neural network and geometric constraint for image-based indoor localization," *IEEE Robot. Autom. Lett.*, vol. 7, no. 2, pp. 1674–1681, Apr. 2022, doi: 10.1109/LRA.2022.3140832.
[25] K. Ngamakeur, S. Yongchareon, J. Yu, and Q. Z. Sheng, "Deep CNN-LSTM network for indoor location estimation using analog signals of passive infrared sensors," *IEEE Internet Things J.*, vol. 9, no. 22, pp. 22582–22594, Nov. 2022, doi: 10.1109/JIOT.2022.3183148.
[26] X. Liu, J. Cen, Y. Zhan, and C. Tang, "An adaptive fingerprint database updating method for room localization," *IEEE Access*, vol. 7, pp. 42626–42638, 2019, doi: 10.1109/ACCESS.2019.2908000.
[27] Y. Chen and A. Terzis, "On the implications of the log-normal path loss model: An efficient method to deploy and move sensor motes," in *Proc. 9th ACM Conf. Embedded Networked Sensor Syst.*, Nov. 2011, pp. 26–39, doi: 10.1145/2070942.2070946.
[28] F. U. Khan, M. Awais, M. B. Rasheed, B. Masood, and Y. Ghadi, "A comparison of wireless standards in IoT for indoor localization using LoPy," *IEEE Access*, vol. 9, pp. 65925–65933, 2021, doi: 10.1109/ACCESS.2021.3076371.
[29] S. Sadowski and P. Spachos, "RSSI-based indoor localization with the Internet of Things," *IEEE Access*, vol. 6, pp. 30149–30161, 2018, doi: 10.1109/ACCESS.2018.2843325.
[30] H. Kausar and S. Chattaraj, "A novel Kalman filter based trilateration approach for indoor localization problem," in *Proc. Int. Conf. for Advancement Technol. (ICONAT)*, Jan. 2022, pp. 1–5, doi: 10.1109/ICONAT53423.2022.9725834.
[31] D. J. Suroso, M. Arifin, and P. Cherntanomwong, "Distance-based indoor localization using empirical path loss model and RSSI in wireless sensor networks," *J. Robot. Control*, vol. 1, no. 6, pp. 199–207, 2020, doi: 10.18196/jrc.1638.
[32] K. Yang, Z. Liang, R. Liu, and W. Li, "RSS-based indoor localization using min-max algorithm with area partition strategy," *IEEE Access*, vol. 9, pp. 125561–125568, 2021, doi: 10.1109/ACCESS.2021.3111650.
[33] J. Blumenthal, R. Grossmann, F. Golatowski, and D. Timmermann, "Weighted centroid localization in zigbee-based sensor networks," in *Proc. IEEE Int. Symp. Intell. Signal Process.*, 2007, pp. 1–9, doi: 10.1109/wisp.2007.4447528.
[34] B. T. Chhetri, A. Alsadoon, P. W. C. Prasad, H. S. Venkata, and A. Elchouemi, "Enhanced weighted centroid localization in RFID technology: Patient movement tracking in hospital," in *Proc. 5th Int. Conf. Adv. Comput. Commun. Syst. (ICACCS)*, Mar. 2019, pp. 910–915, doi: 10.1109/ICACCS.2019.8728552.
[35] B. S. Hantono, A. E. Suryanto, and N. Prastianto, "Testing Bluetooth low energy as indoor positioning technology using measured path loss exponent and weighted centroid localization methods," in *Proc. 14th Int. Conf. Inf. Technol. Electr. Eng. (ICITEE)*, Oct. 2022, pp. 124–129, doi: 10.1109/ICITEE56407.2022.9954072.
[36] Q. Xin and W. Zhang, "Research on law of RSSI fluctuation of wireless sensor networks," in *Proc. 3rd Int. Conf. Comput. Vis., Image Deep Learn. Int. Conf. Comput. Eng. Appl. (CVIDL ICCEA)*, May 2022, pp. 965–968, doi: 10.1109/CVIDLICCEA56201.2022.9825114.
[37] F. A. Abed, Z. A. Hamza, and M. F. Mosleh, "Indoor positioning system based on Wi-Fi and Bluetooth low energy," in *Proc. 8th Int. Eng. Conf. Sustain. Technol. Develop. (IEC)*, Feb. 2022, pp. 136–141, doi: 10.1109/IEC54822.2022.9807489.
[38] W. Li and Y. Jia, "Distributed target tracking by time of arrival and received signal strength with unknown path loss exponent," *IET Signal Process.*, vol. 9, no. 9, pp. 681–686, Dec. 2015, doi: 10.1049/iet-spr.2014.0477.
[39] A. Booranawong, N. Jindapetch, and H. Saito, "An autonomous RSSI filtering method for dealing with human movement effects in an RSSI-based indoor localization system," *J. Electr. Eng. Technol.*, vol. 15, no. 5, pp. 2299–2314, Sep. 2020, doi: 10.1007/s42835-020-00483-w.
[40] J. J. Robles, J. S. Pola, and R. Lehnert, "Extended min-max algorithm for position estimation in sensor networks," in *Proc. WPNC 9th Work. Positioning, Navig. Commun.*, 2012, pp. 47–52, doi: 10.1109/WPNC.2012.6268737.
[41] A. Kaur, P. Kumar, and G. P. Gupta, "A weighted centroid localization algorithm for randomly deployed wireless sensor networks," *J. King Saud Univ. Comput. Inf. Sci.*, vol. 31, pp. 82–91, Jan. 2017, doi: 10.1016/j.jksuci.2017.01.007.
[42] K.-Y. Kim and Y. Shin, "A distance boundary with virtual nodes for the weighted centroid localization algorithm," *Sensors*, vol. 18, no. 4, p. 1054, Apr. 2018, doi: 10.3390/s18041054.
[43] S. Sinha and S. Ashwini, "RSSI based improved weighted centroid localization algorithm in WSN," in *Proc. 2nd Int. Conf. Emerg. Technol. (INCET)*, May 2021, pp. 1–4, doi: 10.1109/INCET51464.2021.9456134.
[44] F. Shang, W. Su, Q. Wang, H. Gao, and Q. Fu, "A location estimation algorithm based on RSSI vector similarity degree," *Int. J. Distrib. Sensor Netw.*, vol. 10, no. 8, Aug. 2014, Art. no. 371350, doi: 10.1155/2014/371350.
[45] P. Keawbunsong, S. Duangsuwan, P. Supanakoon, and S. Promwong, "Quantitative measurement of path loss model adaptation using the least squares method in an urban DVB-T2 system," *Int. J. Antennas Propag.*, vol. 2018, pp. 1–8, 2018, doi: 10.1155/2018/7219618.

FARID YULI MARTIN ADIYATMA received the B.Eng. degree in engineering physics from Universitas Gadjah Mada (UGM), Indonesia, in 2021. He is currently pursuing the Ph.D. degree in robotics and computational intelligence systems with the School of Engineering, King Mongkut's Institute of Technology Ladkrabang (KMITL), Thailand. His research interests include indoor localization, wireless sensor networks, the Internet of Things, and machine learning.

DWI JOKO SUROSO received the B.Eng. degree in engineering physics from Universitas Gadjah Mada (UGM), Indonesia, in 2010, and the master's and Ph.D. degrees from the King Mongkut's Institute of Technology Ladkrabang (KMITL), Thailand, in 2012 and June 2023, respectively. His Ph.D. thesis was focused on using deep generative modeling for radio fingerprinting techniques. From 2014 to 2018, he was a Research Assistant of 5G wireless communication research with the Tokyo Institute of Technology, Japan. Since 2018, he has been a Faculty of engineering physics with UGM. His research interests include short-range wireless communication, including indoor localization and Wi-Fi sensing systems for intelligent and sustainable buildings. Some of his research topics are also integrated with machine and deep learning.

PANARAT CHERNTANOMWONG received the B.Eng. and M.Eng. degrees from the King Mongkut's Institute of Technology Ladkrabang (KMITL), Thailand, in 1998 and 2000, respectively, and the D.Eng. degree from the Tokyo Institute of Technology, Japan, in 2008. She is currently an Assistant Professor with the School of Engineering, KMITL. Her research interests include wireless and mobile communications, especially localization, improvement of positioning algorithms, the Internet of Things (IoT), and smart systems.